

See discussions, stats, and author profiles for this publication at: <https://www.researchgate.net/publication/234923384>

Modeling high power light-emitting diode spectra and their variation with junction temperature

Article in Journal of Applied Physics · August 2010

DOI: 10.1063/1.3463411

CITATIONS

58

READS

700

4 authors:



Arno Keppens

Belgian Institute for Space Aeronomy

69 PUBLICATIONS 471 CITATIONS

[SEE PROFILE](#)



W. R. Ryckaert

KU Leuven

77 PUBLICATIONS 1,157 CITATIONS

[SEE PROFILE](#)



Geert Deconinck

KU Leuven

455 PUBLICATIONS 4,611 CITATIONS

[SEE PROFILE](#)



Peter Hanselaer

KU Leuven

172 PUBLICATIONS 1,793 CITATIONS

[SEE PROFILE](#)

Some of the authors of this publication are also working on these related projects:



EMPIR JRP 18SIB03 - New Quantities for the Measurement of Appearance (BxDiff) [View project](#)



Modelling and evaluation of high power LEDs for general lighting [View project](#)

Modeling high power light-emitting diode spectra and their variation with junction temperature

A. Keppens,^{1,2,a)} W. R. Ryckaert,^{1,2} G. Deconinck,² and P. Hanselaer^{1,2}

¹*Light and Lighting Laboratory, Catholic University College Gent, Gebroeders Desmetstraat 1, B-9000 Gent, Belgium*

²*ESAT/ELECTA, K.U.Leuven, Kasteelpark Arenberg 10, B-3001 Leuven, Belgium*

(Received 22 January 2010; accepted 16 June 2010; published online 20 August 2010)

Spectral radiant flux is the primary optical characteristic of a light source, determining the luminous flux and color. Much research is dedicated to the modeling of light-emitting diode (LED) spectra and their temperature dependence, allowing for the simulation of optical properties in various applications. Most of the spectral radiant flux models that have been published so far are purely mathematical. For this paper, spectral radiant fluxes of commercial single color LED packages have been measured in a custom made integrating sphere at several junction temperatures by active cooling and heating with a Peltier element. A spectrum model at 300 K is constructed where the Boltzmann free carrier distribution and carrier temperature are included. Subsequently, the model is extended with the carrier temperature variation, the band gap energy shift, and the nonradiative recombination rate decrease with junction temperature. As a result, the skewness variation, peak frequency shift, and peak value change in the spectrum with temperature can be predicted. The model has been validated by comparing flux and color coordinates of measured and simulated spectra at 340 K junction temperature. In practice, only two spectral flux measurements at different junction temperatures are needed to accurately simulate a single color spectrum at any temperature.

© 2010 American Institute of Physics. [doi:[10.1063/1.3463411](https://doi.org/10.1063/1.3463411)]

I. INTRODUCTION

The use of light-emitting diodes (LEDs) has become very popular in decorative lighting and signalization applications but a breakthrough in general lighting has not been achieved yet. Main obstacles are the moderate system efficiency and luminous flux. Furthermore, optical and electrical characteristics are strongly dependent on the diode junction temperature, which in turn is determined by the forward current, heat sink, and ambient temperature.

The spectral radiant flux is the primary LED optical characteristic, determining luminous flux and color. A lot of effort has been attributed to model the LED spectral flux and its variation with junction temperature.

One of the first attempts consisted of a rather simple LASTIP simulation of previously measured LED and laser spectra.¹ In 2005 however, a Gaussian spectrum model appeared more successful² and this model simplified incorporation of the peak wavelength variation with junction temperature.³ Very soon afterwards, a double Gaussian model was presented,⁴ which is nowadays still used for lighting calculations by the International Commission on Illumination (CIE). A more general approach based on the double Gaussian model was published in 2006.⁵ In 2008 a variant of the split Gaussian function with a different exponential behavior on each side of the maximum was reported to be a more simplified approach, still containing the junction temperature as a free parameter.⁶ More recently an evaluation of several LED spectrum approximations has been published⁷ but due to the large number of fitting parameters an easy-to-use modeling approach is not provided. Furthermore, most

spectral radiant flux models that have been published so far are purely mathematical and any link with underlying physical principles is missing. Moreover, integration of the junction temperature variation into the initial model parameters often results in piecewise defined and complex models.

In this paper, a spectrum model is constructed where the Boltzmann exponential behavior with carrier temperature variation, band gap energy shift, and the increase in the non-radiative recombination rate with junction temperature are included explicitly. In a first step, an experimental spectrum at a particular temperature is modeled with two exponentials and a Gaussian function, using frequency as the main variable. Afterwards, peak frequency, absolute spectrum power, and spectrum skewness variation with temperature are implemented. The model allows for very accurate simulations of single color LED spectra at any temperature.

II. EXPERIMENTS

Red (R), green (G), and blue (B) commercial LED packages have been selected from two manufacturers. A nominal drive current of 350 mA was selected, resulting in an input power of about 1 W. The junction temperature was determined according to the forward voltage method described before.^{8,9} The packaged LEDs were placed in a Heraeus UT6 isothermal oven with active air circulation. Four following temperatures have been selected within a range of typical LED operation temperatures: 300, 320, 340, and 360 K. These predefined temperatures have been precisely measured with a PT100 thermistor, four-wire connected with a Keithley 2510 TEC SourceMeter. For each setting, at least 20 min delay between the set-temperature and the measurement was respected in order to assure thermal equilibrium between

^{a)}Electronic mail: arno.keppens@kahosl.be.

the air in the oven and the diode junction. Thermal equilibrium was checked by measuring the forward voltage at a small current (1 mA) every two minutes. Voltage measurements were performed with a Keithley 2440 5A SourceMeter used in a four-wire set-up and controlled by a LABVIEW 7.1 program. Once the thermal equilibrium had been reached, a pulse of a few milliseconds at 350 mA normal drive current was applied and the forward voltage during the pulse was measured. Successive voltage measurements indicate that junction temperature increase in the LED die during these measurements can be neglected.

The voltages measured during the 350 mA pulses at different oven temperatures resulted in a calibration curve between diode forward voltage at 350 mA current and junction temperature. From this calibration curve the junction temperature of the LEDs during spectral radiant flux measurements at constant 350 mA current could be determined. The flux was measured with a custom made integrating sphere with particular location of the reference port, detection port and sample port.¹⁰ A quartz fiber bundle (3 mm diameter) couples the light into a 1/4 m focal length spectrometer (Oriol Instruments type 74055 MS260i). The grating has a line density of 150 lines/mm. At the spectrometer exit plane, a 1 in. Andor back illuminated and cooled (-30°C) charge coupled device detector (model iDUS DV420A-BU2) is mounted, resulting in a spectral resolution of approximately 4 nm while the complete visible spectrum is recorded. Data acquisition with full vertical binning, dark current correction and an integration time set for optimum signal-to-noise ratio is controlled by LABVIEW software.

Each LED package has been attached to the sphere surface using an aluminum mounting plate incorporating a Peltier element and a PT100 thermistor, four-wire connected with a Keithley 2510 TEC SourceMeter. The Peltier element (with active air cooling) regulates the plate temperature until the thermistor shows the same temperature as the Keithley set point temperature. Meanwhile, junction temperature is determined using the voltage-temperature calibration. Because of the thermal resistance between the LED junction and the mounting plate,¹¹ the thermistor set point temperature must be lowered until the diode junction temperature reaches the desired value. The total spectral radiant flux has been measured for each package at five junction temperatures selected between 290 and 340 K.

III. SINGLE COLOR SPECTRUM MODEL

Two typical experimental single color LED spectra for the same LED at two junction temperatures are shown in Fig. 1. With increasing temperature, a decrease in peak value and an increase in peak wavelength and skewness can be observed.

In theory, the photon energy distribution of a LED is determined by the product of the density of energy states within the allowed energy band and a Boltzmann energy distribution.¹² The Boltzmann distribution is proportional to $\exp(-E/kT_c)$, i.e., the energy distribution of a charge carrier gas of electrons and holes at a carrier temperature T_c . This carrier temperature is typically higher than the diode junction

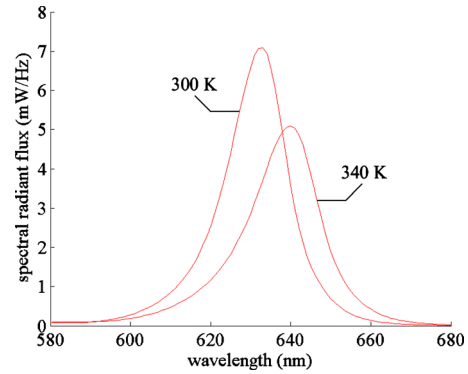


FIG. 1. (Color online) Experimental spectra of LED R1 at two different junction temperatures.

temperature T .¹² On the other hand, the density of energy states above E_g is proportional to $(E - E_g)^{1/2}$. One can easily show that the product of these expressions has its maximum at $E_g + kT_c/2$, with k the Boltzmann constant. From these theoretical considerations, it seems more appropriate to examine LED spectra taking energy or frequency as the main parameter ($E = h\nu$ with h the Planck constant) and using a logarithmic scale.¹³ This is illustrated in Fig. 2.

In Fig. 2, the Boltzmann exponential behavior beyond the peak frequency can be easily recognized and the slope decrease with junction temperature can be predicted as well. The spectrum's full width at half maximum (FWHM) and its temperature dependence are determined by both slopes. However, the sharp spectrum cut-off at the low energy side of the peak frequency as predicted by theory is not observed. The measured spectra show an exponential behavior even on the low energy slope. Analogous results have been reported in literature^{3,14} and have been attributed to thermal agitation of the diode's crystal lattice.¹⁵ This behavior justifies the construction of a spectrum model using frequency as variable and starting from an exponential behavior on both sides of the spectrum peak. A first modeling attempt containing a combination of two exponentials has been given by:⁶

$$\Phi_{e,\lambda} = \frac{2S_0}{\exp\left[\frac{\lambda - \lambda_p}{B(\lambda)}\right] + \exp\left[-\frac{\lambda - \lambda_p}{B(\lambda)}\right]}, \quad (1)$$

with S_0 the spectral intensity at the peak wavelength λ_p and $B(\lambda)$ a piecewise defined asymmetrical line width. It is how-

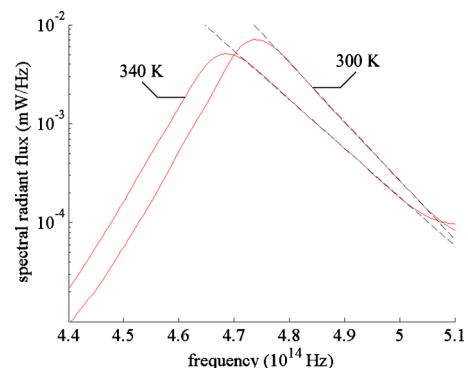


FIG. 2. (Color online) Experimental spectra of LED R1 on a logarithmic scale and with frequency as main variable. The dashed lines show the Boltzmann exponential behavior.

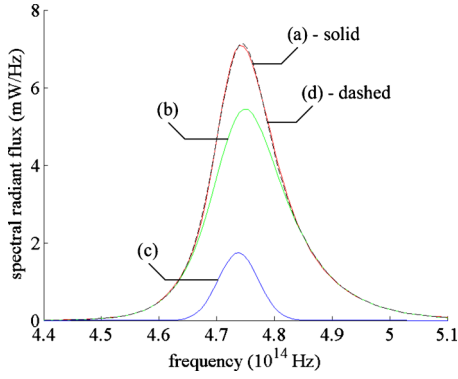


FIG. 3. (Color online) The solid line (a) corresponds with the measured spectrum. The line (b) represents the spectrum model according to Eq. (2), while the line (c) represents the Gaussian fit of the difference between (a) and (b). The dashed line (d) is the simulated spectrum according to the model of Eq. (3).

ever clear that the spectrum model in Eq. (1) lacks any physics-based background. In order to insert the Boltzmann behavior explicitly, this equation has been adapted as follows:

$$\Phi_{e,\nu} = \frac{1}{S_1 \exp[-a(\nu - \nu_p)] + S_2 \exp\left[\frac{h}{kT_c}(\nu - \nu_p)\right]}, \quad (2)$$

with ν_p the experimental peak frequency and S_1 , S_2 , a , and T_c four positive fitting parameters. Expression (2) does not contain any piecewise defined parameters anymore. In practice, S_1 and a on one hand and S_2 and T_c on the other hand are determined from two separate exponential fits to the low energy and high energy tail of the diode spectrum, respectively.

An experimental diode spectrum at 300 K constant junction temperature is plotted in Fig. 3, together with the simulation based on Eq. (2). This plot shows that the exponential behavior described by Eq. (2) is not able to model the com-

plete spectrum shape. However, the difference between the experimental curve and the curve according to Eq. (2) can be approximated by a Gaussian function. Therefore, a Gaussian function is added, resulting in the following analytical model:

$$\Phi_{e,\nu} = \frac{1}{S_1 \exp[-a(\nu - \nu_p)] + S_2 \exp\left[\frac{h}{kT_c}(\nu - \nu_p)\right] + S_3 \exp\left[-\left(\frac{\nu - \nu_G}{b}\right)^2\right]}, \quad (3)$$

with S_3 , b and the peak frequency of the Gaussian function (ν_G) acting as three additional parameters. Equation (3) can be considered a variant of the double Gaussian model presented by Ohno.⁴

Although seven parameters have to be determined for the description of a diode spectrum, the fitting approach is still very basic. Two parameters are determined from each tail of the spectrum resulting in Eq. (2). After subtraction of this equation from the measured spectrum, a Gaussian fit provides the remaining three parameters.

The spectrum model as described by Eq. (3) has been applied to all devices at a constant junction temperature of 300 K. The corresponding fitting parameters have been collected in Table I.

As expected, T_c values are always higher than the junction temperature, while ν_G values are found close to the peak frequency ν_p . It is interesting to note that for most of the fitting parameters the values obtained for AlGaInP-based LEDs (red) can be distinguished from the values obtained for InGaN-based emitters (green and blue). The values of T_c , a , and b show that the spectrum's FWHM, which typically equals a few kT_c , is larger for InGaN emitters. This may be due to a higher forward voltage and high-energy injection of carriers into the active region.¹⁶ As a consequence, the values of S_3 switch from positive for AlGaInP based LEDs to nega-

TABLE I. Experimental peak frequencies and fitting parameters for all LEDs at $T=300$ K. Coefficients of determination R^2 have been added for the Gaussian fits. For the exponential fits all R^2 values exceed 0.99.

LED	ν_p (10^{14} Hz)	S_1^{-1} (mW)	a (10^{-14} Hz $^{-1}$)	S_2^{-1} (mW)	T_c (K)
R1	4.736	73.450	22.556	126.200	369.8
R2	4.738	10.676	22.370	14.022	322.8
G1	5.701	4.152	7.378	2.248	421.8
G2	5.799	9.277	6.809	5.819	588.0
B1	6.664	9.741	7.773	19.770	418.2
B2	6.503	30.361	7.971	26.152	481.8
LED	S_3 (mW)	b (10^{14} Hz)	ν_G (10^{14} Hz)	R^2	
R1	1.597	0.051	4.721	0.990	
R2	4.488	0.045	4.731	0.996	
G1	-0.219	0.098	5.585	0.873	
G2	-1.123	0.166	5.724	0.997	
B1	-1.301	0.111	6.697	0.973	
B2	-3.106	0.134	6.468	0.997	

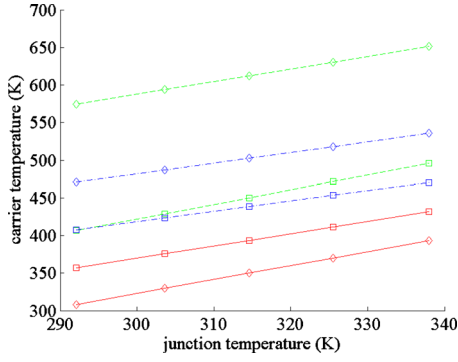


FIG. 4. (Color online) Carrier temperature variation with junction temperature for the solid lines, dashed lines, and dotted-dashed lines diodes. Squares are used for LEDs from manufacturer 1, diamonds are used for devices from manufacturer 2.

tive for InGaN based diode chips. Also the numerical value of the low energy slope seems to be characteristic for each compound semiconductor. The value of a equals about $22.5 \times 10^{-14} \text{ Hz}^{-1}$ for AlGaInP emitters and $7.5 \times 10^{-14} \text{ Hz}^{-1}$ for InGaN diodes.

IV. TEMPERATURE DEPENDENCE OF A SINGLE COLOR SPECTRUM

In the single color spectrum model given by Eq. (3), seven fitting parameters appear: S_1 , a , S_2 , T_c , S_3 , b , and ν_G . In order to examine and include the junction temperature dependence of these parameters, additional spectra have been measured and modeled at four junction temperatures between 290 and 340 K.

A. Variation in exponentials

The variation in the carrier temperature T_c with junction temperature has been found to be approximately linear for typical diode junction temperature ranges.¹³ Our data, summarized in Fig. 4, confirms this behavior for all LED packages under test.

Considering the spectrum at 300 K as a reference spectrum, the carrier temperature variation can be modeled as follows:

$$T_c(T) \approx c(T - T_{ref}) + T_{c,ref} = c\Delta T + T_{c,ref}, \quad (4)$$

where c represents a positive fitting parameter and $T_{c,ref}$ equals the carrier temperature at 300 K junction temperature as given in Table I. The numerical values of slope c are gathered in Table II. With $c > 1$, it is clear that the carrier temperature remains always higher than the junction temperature.

The variation with temperature of fitting parameters a (low energy slope) and b (peak width of the additional Gaussian contribution) occurring in Eq. (3) has been found to be negligible for all single color emitters. This implies that a and b values found in Table I can be used in the spectrum model for the complete temperature range. Moreover, if a and b are constant, the spectral FWHM and skewness variation with temperature must be attributed to the temperature behavior of T_c , which is linear. This offers an explanation for the experimental results reported in literature.^{3,5}

TABLE II. Variation in carrier temperature c , total spectrum's peak frequency (γ_p), and the Gaussian peak frequency (γ_G) with junction temperature, together with the characteristic temperature T_0 . R^2 values exceed 0.95 for all fits.

LED	c	γ_p (10^{14} Hz/K)	γ_G (10^{14} Hz/K)	T_0 (K)
R1	1.630	0.001 304	0.001 152	240.0
R2	1.853	0.001 039	0.001 012	128.7
G1	1.945	0.000 312	0.000 082	258.0
G2	1.677	0.000 270	0.000 253	367.6
B1	1.376	0.000 397	0.000 542	235.3
B2	1.416	0.000 413	0.000 518	225.1

B. Peak frequency shift

All LED spectra show a downward peak frequency shift with junction temperature as illustrated in Figs. 1 and 2. In Fig. 5, the variation in the peak frequencies ν_p and ν_G with junction temperature is plotted for the LED R1. For both parameters a linear decrease is observed, although with a slightly different slope.

The peak frequency shift can be attributed to the variation in the semiconductor's energy gap E_g with temperature, described by the Varshni formula:¹⁷

$$E_g(T) = E_g(0) - \frac{\alpha T^2}{T + \beta}, \quad (5)$$

where α and β are two positive fitting parameters, the so-called Varshni parameters. $E_g(0)$ represents the energy gap for $T=0$ K. For junction temperatures above about 290 K, the Varshni formula may be approximated by a linear expression:⁸

$$E_g(T) \approx E_{g,ref} - \alpha'(T - T_{ref}), \quad (6)$$

with $E_{g,300}$ the band gap energy at 300 K and α' a positive constant. This linear decrease can explain the linear decrease in the peak frequency as presented in Fig. 5. Starting from a reference value at a reference temperature T_{ref} , the position of the peak frequency at any other temperature T can be calculated as:

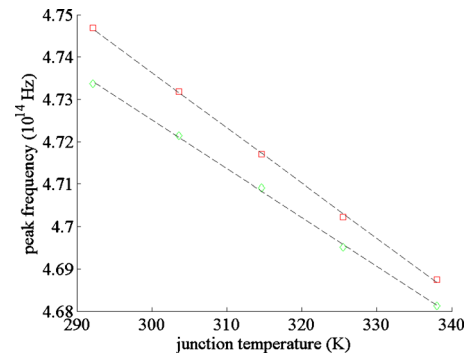


FIG. 5. (Color online) Peak frequency shift (squares) and shift in ν_G (diamonds) with junction temperature for the LED R1. The dashed lines represent linear fits.

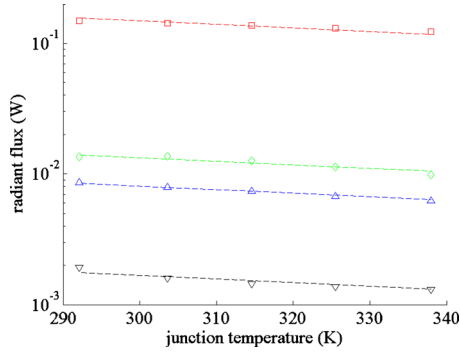


FIG. 6. (Color online) Radiant flux variation with junction temperature of LED R1 for the complete spectrum $\Phi_{e,\nu}$ (squares), S_1^{-1} (diamonds), S_2^{-1} (triangles), and S_3 (inverted triangles). The dashed lines represent exponential fits with the same characteristic temperature.

$$\nu_p(T) \approx \nu_{p,ref} - \gamma_p(T - T_{ref}), \quad (7)$$

with $\gamma_p = \alpha'/h$. For all single color LED spectra, the γ_p values have been summarized in Table II. The values are in accordance with values found in LED datasheets and confirm that the frequency shift for red LEDs is about two to three times higher than the shift for green and blue LEDs. From the values of γ_p , numerical values of α' can be deduced. They agree with values found in literature, and are typically lying between 0.1 and 0.5 meV/K for bulk InGaN and between 0.3 and 0.4 meV/K for bulk AlGaInP compound semiconductors.¹²

From Fig. 5, the relationship between $\nu_G(T)$ and γ_G seems to be completely similar to Eq. (7). Experimental γ_G values are also summarized in Table II. Only for LED G1 γ_G is remarkably different from γ_p . This may have his origin in the rather poor Gaussian fits for this device with R^2 below 0.9 (see Table I for fit at 300 K).

Despite the theoretical and experimental evidence for a linear behavior of the peak frequency with junction temperature given above, in literature most often the peak *wavelength* is considered to change proportionally with temperature.^{16,18,19} Although this approximation is valid within a limited temperature range, it would be more correct to state that $\Delta(\lambda^{-1})$ is proportional to the junction temperature variation.

C. Absolute power variation

From Figs. 2, 4, and 6, it is obvious that the spectral radiant power decreases with increasing junction temperature. At constant forward current, the spectral flux is propor-

tional with the total external quantum efficiency.¹⁵ This total external quantum efficiency equals the product of internal quantum efficiency η_i and extraction efficiency η_{ext} :

$$\Phi_e \propto \eta_i \eta_{ext}. \quad (8)$$

The extraction efficiency majorly depends on the LED chip configuration and is therefore assumed not to change with temperature. The internal quantum efficiency's temperature dependence can be expressed as follows:²⁰

$$\eta_i = \left[1 + \left(\frac{p\tau_i N_i}{n\tau_r N_r} \right) \exp\left(-\frac{E_i - E_r}{kT}\right) \right]^{-1} \quad (9)$$

with n , p , τ_i , N_i , and E_i the electron and hole concentration and lifetimes, concentrations and energies of radiative and nonradiative recombinations, respectively. The indices t and r account for trap and radiative related transitions, respectively.

For practical application temperatures (between about 300 and 400 K), Eq. (9) can be approximated by an exponential decrease with increasing temperature, which can thus be attributed to the increase in nonradiative recombinations. This dependence has also been found experimentally and formulated as:^{3,12}

$$\Phi_e(T) \propto \exp\left(-\frac{T - T_{ref}}{T_0}\right), \quad (10)$$

with T_{ref} a reference temperature. The denominator T_0 is called the characteristic temperature. A high characteristic temperature implies a weak temperature dependence.

In order to check the consistency of Eq. (9) with the model as described by Eq. (3), the fitting parameters S_1^{-1} , S_2^{-1} , and S_3 of LED R1 have been plotted for several junction temperatures in Fig. 6. These three parameters decrease exponentially with temperature. The slopes are more or less identical, suggesting that one common characteristic temperature can be identified. All single color diodes under test have proven to show the same behavior. Their corresponding characteristic temperatures have been collected in Table II. Similar characteristic temperatures have been reported in literature.³ However, the characteristic temperature depends on whether radiant or luminous flux is considered in Eq. (10).

D. Overall single color spectrum model

Combining the previous paragraphs, a semiempirical model for a single color LED spectrum at junction temperature T can be written as follows:

$$\Phi_{e,\nu}(T) \approx \left\{ \frac{1}{S_{1,ref} \exp[-a(\nu - \nu_{p,ref} - \gamma_p \Delta T)] + S_{2,ref} \exp\left[\frac{h(\nu - \nu_{p,ref} - \gamma_p \Delta T)}{k(c\Delta T + T_{c,ref})}\right] + S_{3,ref} \exp\left[-\left(\frac{\nu - \nu_{G,ref} - \gamma_G \Delta T}{b}\right)^2\right]} \right\} \exp\left(-\frac{\Delta T}{T_0}\right), \quad (11)$$

TABLE III. Comparison between measured and simulated flux and CIE color coordinates at 340 K.

LED	Measured			Simulated			Deviation	
	Flux (lm)	CIE x	CIE y	Flux (lm)	CIE x	CIE y	Flux (%)	ΔE
R1	20.1	0.6939	0.3055	19.6	0.6935	0.3064	2.4	0.0015
R2	26.9	0.6941	0.3053	24.5	0.7037	0.2962	8.9	0.0207
G1	29.2	0.2045	0.6714	28.7	0.2049	0.6844	1.7	0.0028
G2	55.4	0.1671	0.6679	54.7	0.1709	0.6649	1.3	0.0017
B1	4.5	0.1513	0.0284	4.5	0.1511	0.0270	0.0	0.0038
B2	18.0	0.1367	0.0537	17.9	0.1363	0.0534	0.5	0.0007

$\nu_{p,ref}$, $S_{1,ref}$, a , $S_{2,ref}$, $T_{c,ref}$, $\nu_{G,ref}$, $S_{3,ref}$, and b are determined from one reference spectrum at temperature T_{ref} and $\Delta T = T - T_{ref}$. For the determination of γ_p , γ_G , c , and T_0 a spectrum obtained at an additional temperature has to be available.

V. VALIDATION

In order to validate the spectrum model presented in Eq. (11), experimental and simulated spectra of LED R1 at 340 K junction temperature are shown in Fig. 7. The measured spectrum at 300 K has been used as a reference spectrum. c , γ_p , γ_G , and T_0 were determined from Table II. An excellent agreement between simulation and measurement with R^2 exceeding 0.95 has been found.

Additionally, luminous flux and CIE color coordinates at 340 K have been calculated from the simulated spectra and compared with measured data for all LEDs in Table III.

The results in Table III confirm the good agreement between simulation and experiment for all packages under consideration. Except for LED R2, the deviation between simulated and measured luminous flux is smaller than 2.5% and all CIE- $u'v'$ color differences $\Delta E = \sqrt{(\Delta u')^2 + (\Delta v')^2}$ remain significantly smaller than the typical radius of a three-step MacAdam ellipse ($\Delta E \approx 0.006$).²¹ The larger deviations for device R2 might be due to a small bump in the spectrum close to 5×10^{14} Hz. Such spectrum deficiencies are of course not incorporated into the model.

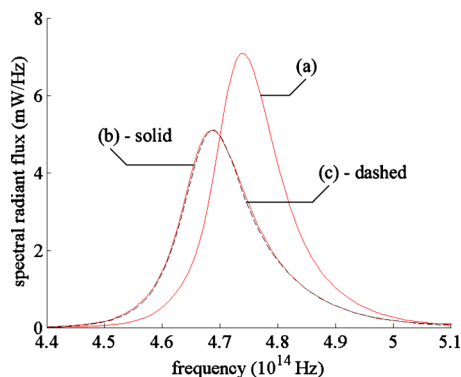


FIG. 7. (Color online) Comparison of measured and simulated spectra for LED R1 at 340 K, starting from a reference spectrum measured at 300 K. The solid line (b) is the measured spectrum at 340 K, while the dashed line (c) is the simulated single color spectrum.

VI. CONCLUSIONS

The spectral radiant flux of six commercial high power LED packages from two manufacturers has been measured with a custom made integrating sphere at different junction temperatures, ranging between 290 and 340 K. A spectrum model for one particular temperature (300 K) has been constructed. Afterwards, the variation in all initial modeling parameters with junction temperature has been examined. In contrast with a number of merely mathematical spectrum models proposed in literature, the Boltzmann exponential behavior with carrier temperature variation, the band gap energy shift and the decrease in the nonradiative recombination rate with junction temperature have been included explicitly. Very high coefficients of determination have been found, indicating a good agreement between the model and measurement data. For most of the fitting parameters the values obtained for AlGaInP-based LEDs could be distinguished from the values obtained for InGaIn-based emitters. The model has been validated by comparing flux and color coordinates of measured and simulated spectra at 340 K junction temperature. Except for one LED showing a spectrum deficiency, flux and color deviations between measurement and simulation have been found to be lower than 2.5% and smaller than the radius of a three-step MacAdam ellipse, respectively. In practice, only two spectral flux measurements are needed to accurately simulate a single color spectrum at any temperature.

ACKNOWLEDGMENTS

The authors, and especially A.K., would like to thank the Belgian divisions of EREA, Massive (Network Philips Consumer Luminaires), R-Tech (Schröder group), and Sylvania for their financial research support.

¹Y.-K. Kuo, J.-Y. Chang, K.-K. Horng, Y.-L. Huang, Y. Chang, and H.-C. Huang, *Proc. SPIE* **4078**, 579 (2000).

²Y. Uchida and T. Taguchi, *Opt. Eng.* **44**, 124003 (2005).

³S. Chhajed, Y. Xi, Y.-L. Li, T. Gessman, and E. F. Schubert, *J. Appl. Phys.* **97**, 054506 (2005).

⁴Y. Ohno, *Opt. Eng.* **44**, 111302 (2005).

⁵K. Man and I. Ashdown, *Proc. SPIE* **6337**, 633702 (2006).

⁶H.-Y. Chou and T.-H. Yang, *J. Light Visual Environ.* **32**, 2 (2008).

⁷F. Reifegerste and J. Lienig, *J. Light Visual Environ.* **32**(3), 288 (2008).

⁸A. Keppens, W. R. Ryckaert, G. Deconinck, and P. Hanselaer, *J. Appl. Phys.* **104**, 093104 (2008).

⁹A. Keppens, D. De Smeyter, W. R. Ryckaert, G. Deconinck, and P. Hanselaer, *Proc. SPIE* **7058**, 70580H (2008).

¹⁰P. Hanselaer, A. Keppens, S. Forment, W. R. Ryckaert, and G. Deconinck,

- [Meas. Sci. Technol.](#) **20**, 095111 (2009).
- ¹¹L. Jayasinghe, Y. Gu, and N. Narendran, [Proc. SPIE](#) **6337**, 63370V (2006).
- ¹²E. F. Schubert, *Light-Emitting Diodes*, 2nd ed. (Cambridge University Press, Cambridge, 2006).
- ¹³Z. Vaitonis, P. Vitta, and A. Zukauskas, [J. Appl. Phys.](#) **103**, 093110 (2008).
- ¹⁴Th. Gessmann, E. F. Schubert, J. W. Graff, K. Streubel, and C. Karnutsch, [IEEE Electron Device Lett.](#) **24**, 683 (2003).
- ¹⁵Y. Deshayes, L. Bechou, F. Verdier, and Y. Danto, [Qual. Reliab. Eng. Int](#) **21**, 571 (2005).
- ¹⁶Y. Xi, J.-Q. Xi, T. Gessmann, J. M. Shah, J. K. Kim, E. F. Schubert, A. J. Fischer, M. H. Crawford, K. H. A. Bogart, and A. A. Allerman, [Appl. Phys. Lett.](#) **86**, 031907 (2005).
- ¹⁷Y. P. Varshni, [Physica \(Amsterdam\)](#) **34**, 149 (1967).
- ¹⁸E. Hong and N. Narendran, [Proc. SPIE](#) **5187**, 93 (2004).
- ¹⁹J. Cho, C. Sone, Y. Park, and E. Yoon, [Phys. Status Solidi A](#) **202**, 1869 (2005).
- ²⁰V. Schwegler, M. Seyboth, S. Schad, M. Scherer, C. Kirchner, M. Kamp, U. Stempfle, W. Limmer, and R. Sauer, MRS Symposia Proceedings No. F99 (Materials Research Society, Pittsburgh, 1999), p. W11.18.
- ²¹CIE, Technical Report—Colorimetry, CIE 15:2004 (2004).